Heat generation when forming AHSS: experimental and numerical analysis of tensile and draw-bead tests

IOP Conf. Series: Materials Science and Engineering **967** (2020) 012086 doi:10.1088/1757-899X/967/1/012086

Heat generation when forming AHSS: experimental and numerical analysis of tensile and draw-bead tests

D M Neto[1], J R Barros[1], M C Oliveira[1], P V Antunes[1], A Ramalho[1], R L Amaral[2], A D Santos[2] and J L Alves[3] and L F Menezes[1]

[1] CEMMPRE, Department of Mechanical Engineering, University of Coimbra, Polo II, Rua Luís Reis Santos, 3030-788 Coimbra, Portugal
[2] Faculty of Engineering, University of Porto, Rua Dr. Roberto Frias,4200-465 Porto, Portugal
[3] CMEMS, Department of Mechanical Engineering, University of Minho, Campus de Azurém, 4800-058 Guimarães, Portugal

E-mail: diogo.neto@dem.uc.pt

Abstract. The increasing use of advanced high-strength steels in sheet metal forming processes requires improved knowledge concerning the thermal and contact conditions. This study presents the experimental and numerical analysis of tensile and draw-bead tests, considering a dual phase steel DP780. The temperature evolution was measured in both tests using an infrared thermal camera. The presented finite element model considers both the heat generated by plastic deformation and friction, as well as the heat loss to the environment by free convention and the contact conductance. The temperature rise in the uniaxial tensile test is accurately predicted by the numerical model. Regarding the draw-bead test, the pulling force is accurately predicted but the temperature variation is overestimated, requiring further investigation.

1. Introduction

Sheet metal forming is a manufacturing process widely used for making shaped components, from soda cans to automotive car bodies. Finished products have good quality, are geometrically accurate and are ready to be used. However, sheet metal forming processes are complex and require expensive tooling, which is economically feasible only for mass production [1]. Advanced High Strength Steels (AHSS) are replacing conventional steels in the production of sheet components, particularly in the automotive industry [2], due to their excellent weight to strength ratio. The high specific strength guarantees the safety and weight reduction requirements, assuring savings in the fuel consumption. However, AHSS present high yield strength and are susceptible to surface damage like adhesion [3], since their deformation involves higher contact pressures than those required by conventional steels.

The frictional conditions at the interface between the forming tools and the metal sheet may vary significantly during the deformation process. Besides, the frictional force depends on diverse parameters such as lubrication, normal pressure, surface roughness of the tool and sheet metal, sliding speed and temperature [4]. Thus, different tribological tests have been developed to model the friction conditions, which can be divided into two categories: (i) process tests and (ii) simulative tests [5]. Process tests comprise typical forming operations without changing the basic process kinematics, while simulative tests reproduce the tribological conditions of forming processes to study friction and/or lubrication. Most of these tests allow the indirect evaluation of the coefficient of friction based on the measurement of

other physical parameters, such as strains or forces [6]. The most frequently applied simulative tests for sheet metal forming can be categorized according to the conditions arising in each region of the forming tool. The conditions in the flange region are usually represented by the strip drawing test, the draw-bead test, and the drawing with tangential compression.

The main function of the draw-beads is to increase the material flow resistance around the periphery of the part, changing the curvature of the metallic sheet passing the draw-bead. The sheet is subjected to multiple bending-unbending when passing through a draw-bead, generating a reverse tension-compression loading over the sheet thickness. The draw-bead test was developed by Nine [7] to model the friction conditions in draw-beads used in sheet metal forming processes. The draw-bead test enables to separate the deformation resistance from the frictional resistance, comparing the values of the pulling and the clamping forces when pulling the strip over fixed and rotating rollers (no frictional resistance). Thus, when the wrap angle of the middle roller is 180º, the coefficient of friction can be calculated through the difference in the drawing force obtained for the rotating and the fixed rollers.

This study explores the potential of using the draw-bead test to evaluate the mechanical and tribological behavior of an AHSS, including the heat generated by plastic deformation and friction. The equipment used was designed to enable the tests to be performed in a tensile test machine and it allows changing the draw-bead penetration depth and gap distance, as well as the pulling speed of the grip. The material considered is a dual phase steel DP780 steel with an initial thickness of 0.8 mm. The experimental tests were performed considering different values of pulling speed. The results include the evolution of the pulling force, as well as the specimen's temperature, which was acquired using an infrared thermal camera. The same procedure was used to evaluate the temperature evolution in the uniaxial tensile test. The thermomechanical models of both tests were built, taking into account the heat generated by plastic deformation and friction, as well as the heat losses to the environment by free convention and due to the contact conductance with the forming tools.

2. Experimental procedure

The uniaxial tensile test was performed along the rolling direction according to ASTM E8M [8] at room temperature with constant crosshead speed (1.3 mm/s), resulting in an initial strain rate of 1.6×10^{-2} s^{-1}. The specimen surface was coated with matt black paint (ensuring an emissivity close to 1) to improve the temperature field measurement with an infrared thermographic camera.

The draw-bead test is essentially composed by four rollers (see Figure 1), which are placed to induce plastic deformation on a sheet strip. The process is divided in three phases: (i) the strip is bended by the middle roller; (ii) the strip is pulled by a grip and (iii) the deformed strip springback. All rollers have 21 mm of diameter, while the dimensions of the sheet strip are 450×25×0.8 mm. Regarding the process parameters, the full penetration was considered (p=21.8 mm), the side clearance between rollers was c=1.55 mm and the total pulling displacement (at constant speed) was 200 mm. In order to maximize the heat generated by friction, the tests were carried out without lubrication. Figure 2 shows the equipment mounted in a tensile test apparatus. The evolution of the middle roller and grip forces was evaluated and the temperature field of the strip was measured with a thermographic infrared camera (FLIR A325), using an image resolution of 320×240 pixels matrix, at 60 frames/s.

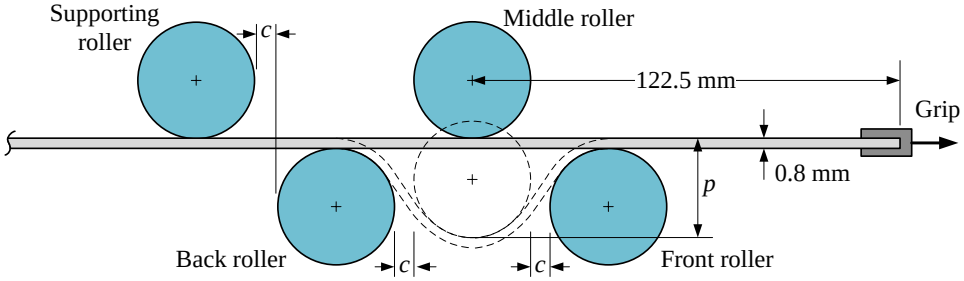

Figure 1. Scheme of the draw-bead test (initial position), composed by four rollers and the strip. The penetration is denoted by p, while the side clearance between rollers is represented by c.

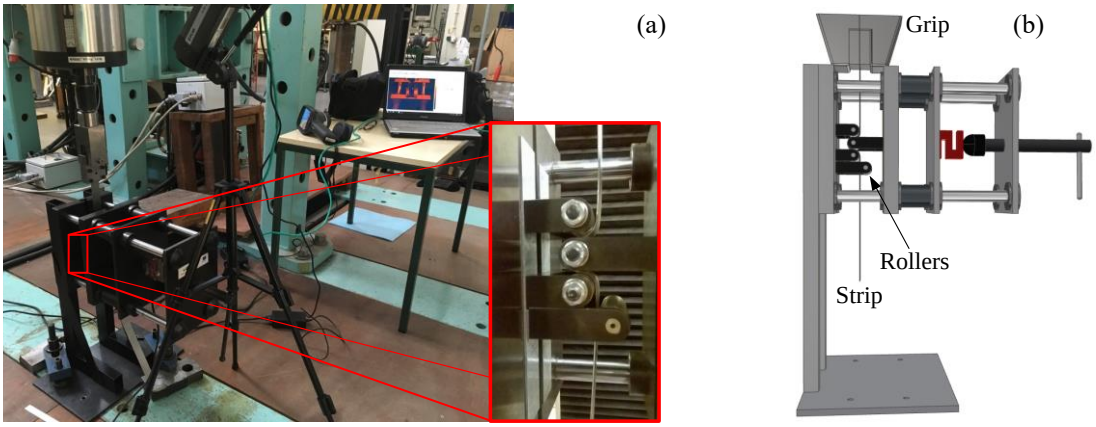

Figure 2. Setup of the draw-bead test: (a) draw-bead equipment in a uniaxial tensile apparatus for large specimen tests and infrared thermal camera; (b) 3D representation of the draw-bead equipment.

3. Numerical model

The transient thermo-mechanical analysis of both tests (uniaxial tensile and draw-bead) was carried out with the in-house implicit finite element code DD3IMP [9], which has been continuously developed for sheet metal forming simulation. The forming tools are assumed rigid and isothermal [10], while the elastoplastic behavior of the dual phase steel DP780 is assumed as temperature independent. The thermo-mechanical coupling was performed through a staggered algorithm [11], which is assumed unidirectional in this study, i.e. the mechanical behavior is independent of the temperature distribution.

The specimens are discretized with 3D linear hexahedral finite elements, using full integration in the thermal analysis and selective reduced integration in the mechanical problem. Three layers of finite elements are adopted in the thickness direction of the strip, to accurately capture the through-thickness gradients. The element size in the length direction is approximately 0.27 mm, i.e. the strip is discretized with 4167 elements. The friction between the strip and the rollers is defined by the Coulomb friction law, using a constant value for the friction coefficient, evaluated by fitting numerical and experimental force evolutions.

3.1. Thermal analysis

The differential equation that defines the thermal conduction within a solid is given by:

$$\rho c_{\mathrm{p}} \frac{\partial T}{\partial t} - k\left(\frac{\partial^2 T}{\partial x^2} + \frac{\partial^2 T}{\partial y^2} + \frac{\partial^2 T}{\partial z^2}\right) - \dot{q}_{\mathrm{p}} - \dot{Q}_{\mathrm{f}} = 0, \tag{1}$$

where ρ is the mass density, c_{p} is the specific heat capacity and k is the thermal conductivity. The thermal properties of the dual phase steel DP780 are: ρ=7900 Kg/m^3, c_{p}=450 J/(KgK) and k=50 W/(mK). The thermal power generated by plastic deformation is defined as the fraction of plastic power converted into heat, given by:

$$\dot{q}_{\mathrm{p}} = \beta \dot{w}^{\mathrm{p}} = \beta(\boldsymbol{\sigma} : \dot{\boldsymbol{\varepsilon}}^{\mathrm{p}}), \tag{2}$$

where β is the Taylor–Quinney factor, $\boldsymbol{\sigma}$ is the Cauchy stress tensor and $\dot{\boldsymbol{\varepsilon}}^{\mathrm{p}}$ is the plastic strain rate tensor. In this study, β is assumed constant and equal to 0.9 [12]. The thermal power generated by the friction forces can be expressed as:

$$\dot{Q}_{\mathrm{f}} = \eta(\mathbf{t}_{\mathrm{t}} \cdot \dot{\mathbf{g}}_{\mathrm{t}}), \tag{3}$$

where η defines the partition of heat dissipated to the strip, $\mathbf{t}_{\mathrm{t}}$ is the frictional force and $\dot{\mathbf{g}}_{\mathrm{t}}$ denotes the relative tangential slip velocity at the contact interface. In this study, the generated heat is equally

partitioned between the two contacting bodies (strip and rollers), thus η= 0.5. The free convection and the contact conductance, both defined on the surface, are given by:

$$\dot{q}_{conv} = h_{conv}(T - T_{\infty}), \tag{4}$$

$$\dot{q}_{c} = h_{c}(T - T_{roller}) = h_{sup} \exp(-m\, g_{n})(T - T_{roller}), \tag{5}$$

where T_{∞} and T_{roller} are the environment and the rollers temperature, respectively. The heat transfer coefficient in free convection is denoted by h_{conv}, while the interfacial heat transfer coefficient h_c depends on the gap distance between the strip and the roller [13]. Thus, the h_{sup} is the upper threshold value (in contact) and m is a free parameter used to control the rate of decrease. Figure 3 presents the variation of the interfacial heat transfer coefficient with the gap distance, comparing three different values of h_{sup}. These conditions are analyzed since the heat transfer coefficient is strongly dependent on the contact pressure and, consequently, on the contact distance, as reported in several studies [14]. The heat transfer coefficient in free convection is 5 W/m^2·K.

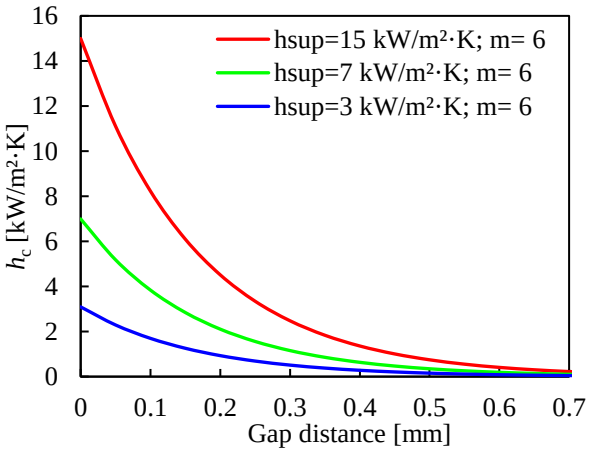

Figure 3. Variation of the interfacial heat transfer coefficient as a function of the normal distance to the roller surface, comparing three different values of upper threshold value.

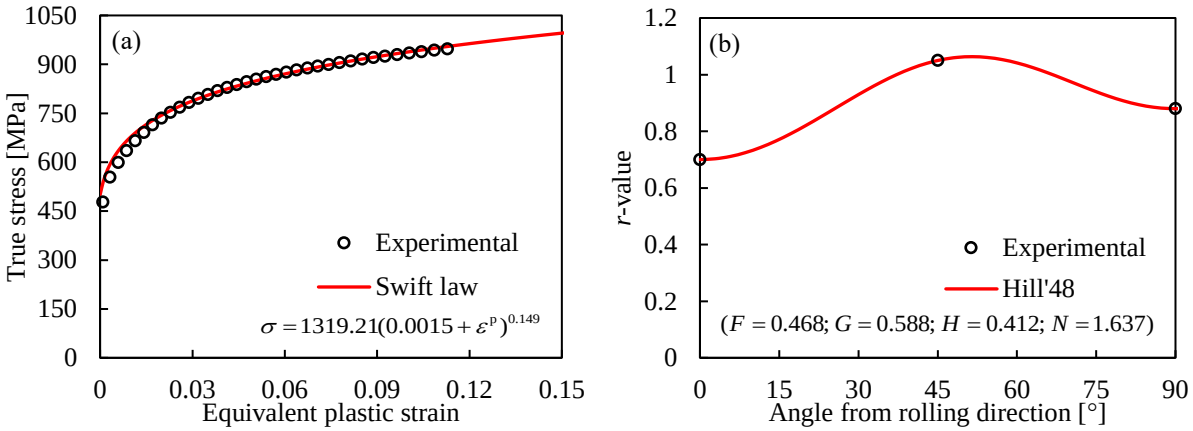

Figure 4. Mechanical behavior of the dual phase steel DP780, comparing the experimental data with the numerical model: (a) true stress–plastic strain curve from the uniaxial tensile test in the rolling direction; (b) evolution of the anisotropy coefficient (r-value) in the plane of the sheet.

3.2. Mechanical analysis

The mechanical behavior of the dual phase steel DP780 is described by an elastoplastic constitutive model. The elastic behavior is assumed isotropic, which is described by the Hooke's law, using 210 GPa for the Young's modulus and 0.30 for the Poisson's ratio. Regarding the plastic behavior, it is described by an isotropic work hardening law (Swift) and a yield criterion (Hill'48). Figure 4 presents the comparison between experimental and numerical results from uniaxial tensile tests. The parameters of the Swift law were calibrated using the stress–strain curve from the uniaxial tensile test with the specimen oriented along the rolling direction (see Figure 4 (a)). The anisotropy parameters of the Hill'48 yield criterion were calibrated using the experimental *r*-values, measured at every 45º from the rolling direction (see Figure 4 (b)).

4. Results and discussion

4.1. Uniaxial tensile test

The transient thermal analysis of the uniaxial tensile test was performed to validate the proposed model, namely the thermal power generated by plastic deformation and the thermal properties of the DP780 steel. The distribution of the predicted temperature variation in the specimen is presented in Figure 5 (a) for three different levels of engineering strain. The comparison between experimental and numerical evolution of the temperature variation in the midpoint of the specimen is presented in Figure 5 (b). The numerical prediction is in good agreement with the experimental measurement, presenting a linear rising up to the onset of necking. Considering the instant of onset of necking, the predicted and experimental temperature rise is about 25ºC and 30ºC, respectively. Although the onset of necking is numerically predicted for a higher value of strain, the rate of the temperature rise after necking is also accurately predicted (see Figure 5 (b)). Thus, the fraction of plastic power converted into heat (90%) and the heat transfer coefficient in free convection (5 W/m^2·K) were accurately selected for this example [12].

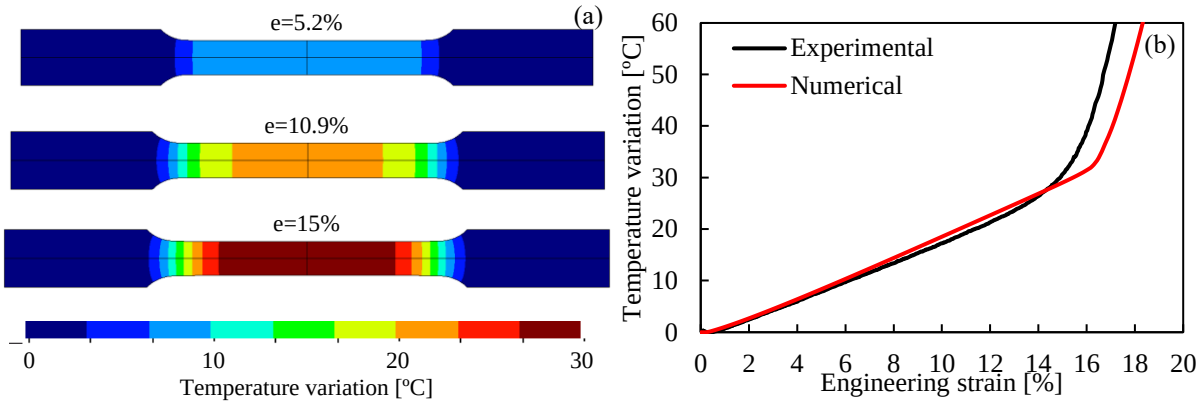

Figure 5. Temperature variation in the uniaxial tensile test considering 1.325 mm/s of crosshead speed: (a) distribution of the predicted temperature variation; (b) comparison between experimental and numerical temperature variation in the midpoint of the specimen.

4.2. Draw-bead test

The experimental tests were performed with different grades of AHSS steels to explore the potential of using the draw-bead test to evaluate the heat generated by plastic deformation and friction. However, due to some restrictions in setting the required laboratory conditions, the experiments were performed with a single sheet strip for each condition. The results are discussed here only for the DP780 considering all available data. The experimental evolution of the pulling force in the draw-bead test is presented in Figure 6 (a), comparing different values of pulling speed. After the initial sheet bending/unbending on the middle roller, the steady state of the pulling force is quickly achieved. There is no evidence that the pulling force is influenced by the pulling speed and even the 30 mm/s curve evolution lies in between

the 15 and 60 mm/s curves, which indicates that the results dispersion corresponds to the level of uncertainty in the measurements. Accordingly, it is assumed that the experimental force evolution is approximately constant during the pulling operation, presenting a value of about 2.5 kN. Also, since the constitutive model adopted to describe the mechanical behavior of the dual phase steel DP780 is not strain rate sensitive (neither temperature sensitive), the predicted pulling force is independent from the pulling speed. Additionally, the influence of the friction coefficient on the numerical pulling force is presented in Figure 6 (b). Considering the frictionless condition (μ=0.0), the predicted pulling force is about 1.5 kN in the steady state regime. On the other hand, the predicted pulling force is close to 2.5 kN for μ=0.12, as highlighted in Figure 6 (b). Comparing experimental and numerical pulling force evolutions, the friction coefficient between the strip and the rollers can be accurately described by a constant value of 0.12.

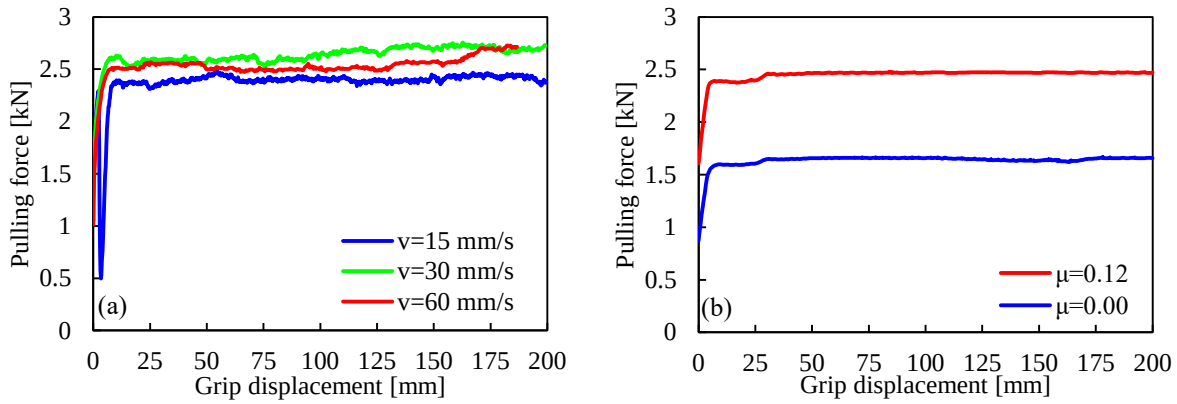

Figure 6. Evolution of the experimental and numerical pulling force: (a) influence of the pulling speed on the experimental force; (b) influence of the friction coefficient on the numerical force.

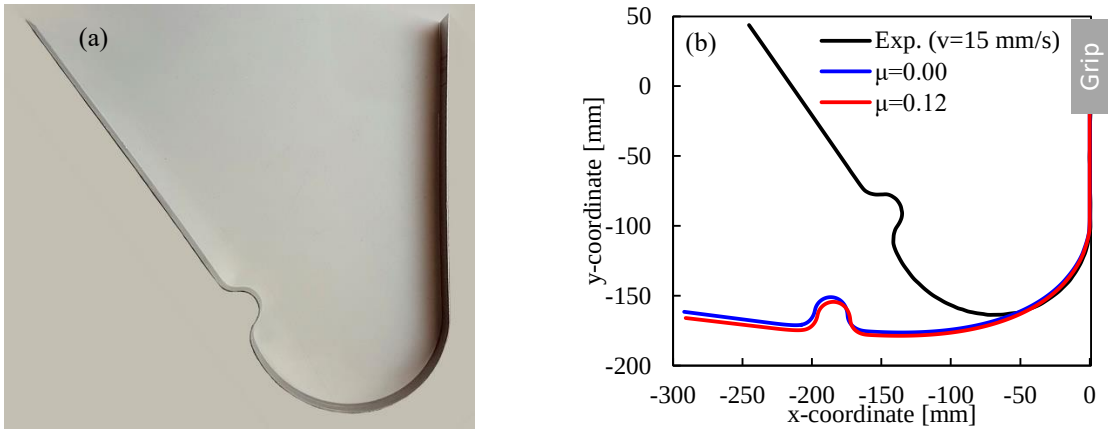

Figure 7. Profile of the strip after springback: (a) the experimental profile obtained for v=15 mm/s; (b) comparison between experimental and numerical profile.

Since the strain rate sensitive of the dual phase steel DP780 is neglected in the numerical model, the predicted final geometry is independent of the pulling velocity and therefore only the experimental condition with a pulling speed v=15 mm/s is considered. The experimental profile of the strip after springback is presented in Figure 7 (a). The curved region of the strip sheet was subjected to multiple bending-unbending induced by the draw-bead geometry. Thus, a decrease of the pulling distance leads to a reduction of the springback. Hence, the accurate assessment of the springback requires the distribution of the turning angle along the section profile [15]. The influence of the friction coefficient on the predicted profile of the strip after springback is presented in Figure 7 (b). Despite the large

influence of the friction coefficient on the predicted pulling force (see Figure 6 (b)), the effect of the friction coefficient on the springback is negligible. Moreover, the springback predicted numerically is significantly lower than the one measured experimentally. This difference can be related with the adoption of an isotropic hardening law. The inclusion of the kinematic hardening can improve the springback prediction since the Bauschinger effect (reduction of the yield stress under reverse loading) is more evident in high strength steels, as well as the pre-strain dependency of the elastic modulus [16]. Indeed, the degradation of elastic stiffness due to plastic straining presents a strong impact on the predicted springback [17]. This may be the main reason why the springback is underestimated.

The thermal analysis of the draw-bead test is presented in Figure 8. The temperature variation at 75 mm ahead the middle roller is presented for three different values of pulling speed. The increase of the pulling speed leads to an increase of the temperature since the time available for the heat loss is lower. Considering the uniaxial tensile test, the influence of the interfacial heat transfer coefficient on the predicted temperature is negligible, since the temperature rise occurs far from the contact zone [12]. Nevertheless, in the draw-bead test, the heat generated by plastic deformation and frictional contact occurs near the contact zone. Thus, three different values of h_{sup} (see Figure 3) were adopted in the draw-bead simulation. The increase of the interfacial heat transfer coefficient leads to a decrease of the temperature rise, as shown in Figure 8 (a), for the lower values considered. The comparison between experimental and numerical temperature variation is presented in Figure 8 (b), considering h_{sup} =15 kW/m^2·K. Despite the large value for the interfacial heat transfer coefficient, the temperature variation is overpredicted by the numerical model, i.e. the numerical prediction of the temperature variation is at least twice the experimental value. The temperature rise is significantly larger in the uniaxial tensile test (Figure 5 (b)) than in the draw-bead test due to the heat lost by contact with the rollers. The frictionless simulation allows to conclude that most of the heat generated comes from plastic deformation.

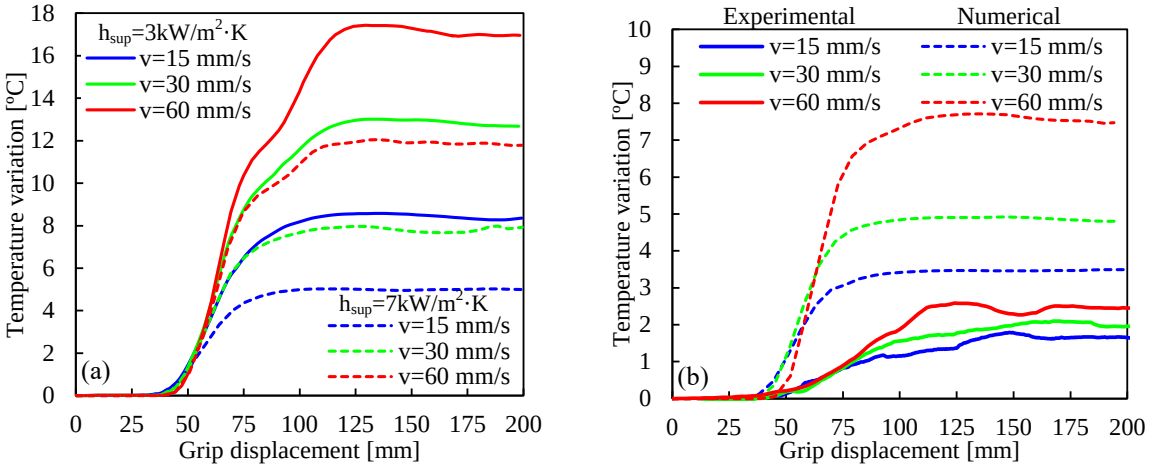

Figure 8. Temperature variation in the draw-bead test ahead the front roller considering different values of pulling speed: (a) influence of the interfacial heat transfer coefficient on the predicted temperature; (b) comparison between experimental and numerical (h_{sup}=15 kW/m^2·K) results.

5. Conclusions

This study presents the experimental and numerical analysis of tensile and draw-bead tests, using the DP780 steel with an initial thickness of 0.8 mm. In addition to the mechanical and tribological behaviour of this steel, the heat generated by plastic deformation and/or friction is evaluated experimentally and numerically. The predicted temperature rise in the uniaxial tensile test is in good agreement with the experimental measurement. Comparing the numerical and experimental results from the draw-bead test, the pulling force is accurately predicted by the numerical model, but the springback is underestimated while the temperature variation is overestimated. The temperature rise is predominantly influenced by the pulling speed, due to the time available for the occurrence of heat losses to the environment by free

convention and the contact conductance with the rollers. Thus, the predicted temperature variation is significantly affected by the adopted interfacial heat transfer coefficient.

Acknowledgments
The authors gratefully acknowledge Prof. Joaquim G. Mendes for the availability of IR thermal equipment used on this research. This work was funded by the Portuguese Foundation for Science and Technology (FCT) under projects with reference PTDC/EME-EME/30592/2017 and PTDC/EME-EME/31657/2017 and by European Regional Development Fund through the Portugal 2020 program and the Centro 2020 Regional Operational Programme (CENTRO-01-0145-FEDER-031657) under the project MATIS (CENTRO-01-0145-FEDER-000014) and UIDB/00285/2020.

References
[1] Ingarao G, Di Lorenzo R and Micari F 2011 Sustainability issues in sheet metal forming processes: an overview *J. Clean. Prod.* **19** 337–47
[2] Lesch C, Kwiaton N and Klose F B 2017 Advanced High Strength Steels (AHSS) for Automotive Applications − Tailored Properties by Smart Microstructural Adjustments *steel Res. Int.* **88** 1700210
[3] Karlsson P, Gåård A, Krakhmalev P and Bergström J 2012 Galling resistance and wear mechanisms for cold-work tool steels in lubricated sliding against high strength stainless steel sheets *Wear* **286**–**287** 92–7
[4] Bay N, Azushima A, Groche P, Ishibashi I, Merklein M, Morishita M, Nakamura T, Schmid S and Yoshida M 2010 Environmentally benign tribo-systems for metal forming *CIRP Ann.* **59** 760–80
[5] Bay N, Olsson D D and Andreasen J L 2008 Lubricant test methods for sheet metal forming *Tribol. Int.* **41** 844–53
[6] Trzepiecinski T and Lemu H G 2019 Recent Developments and Trends in the Friction Testing for Conventional Sheet Metal Forming and Incremental Sheet Forming *Metals (Basel).* **10** 47
[7] Nine H D 1978 Drawbead Forces in Sheet Metal Forming *Mechanics of Sheet Metal Forming* (Boston, MA: Springer US) pp 179–211
[8] ASTM E8 / E8M 2016 Standard Test Methods for Tension Testing of Metallic Materials
[9] Menezes L F and Teodosiu C 2000 Three-dimensional numerical simulation of the deep-drawing process using solid finite elements *J. Mater. Process. Technol.* **97** 100–6
[10] Neto D M, Oliveira M C, Menezes L F and Alves J L 2014 Applying Nagata patches to smooth discretized surfaces used in 3D frictional contact problems *Comput. Methods Appl. Mech. Eng.* **271** 296–320
[11] Martins J M P, Neto D M, Alves J L, Oliveira M C, Laurent H, Andrade-Campos A and Menezes L F 2017 A new staggered algorithm for thermomechanical coupled problems *Int. J. Solids Struct.* **122**–**123** 42–58
[12] Neto D M, Simões V M, Oliveira M C, Alves J L, Laurent H, Oudriss A and Menezes L F 2020 Experimental and numerical analysis of the heat generated by plastic deformation in quasi-static uniaxial tensile tests *Mech. Mater.* **146** 103398
[13] Martins J M, Neto D M, Alves J L, Oliveira M C and Menezes L F 2016 Numerical modeling of the thermal contact in metal forming processes *Int. J. Adv. Manuf. Technol.* **87** 1797–811
[14] Omer K, Butcher C and Worswick M 2020 Characterization of heat transfer coefficient for non-isothermal elevated temperature forming of metal alloys *Int. J. Mater. Form.* **13** 177–201
[15] Neto D M, Oliveira M C, Santos A D, Alves J L and Menezes L F 2017 Influence of boundary conditions on the prediction of springback and wrinkling in sheet metal forming *Int. J. Mech. Sci.* **122** 244–54
[16] Chongthairungruang B, Uthaisangsuk V, Suranuntchai S and Jirathearanat S 2013 Springback prediction in sheet metal forming of high strength steels *Mater. Des.* **50** 253–66
[17] Eggertsen P-A and Mattiasson K 2010 On constitutive modeling for springback analysis *Int. J. Mech. Sci.* **52** 804–18